Polymer 51 (2010) 75–83

Contents lists available at ScienceDirect

Polymer

journal homepage: www.elsevier.com/locate/polymer

Synthesis and characterization of side-chain liquid-crystalline block-copolymers containing laterally attached photoluminescent quinquephenyl units via ATRP

Ling-Yung Wang, Kuang-Chieh Li, Hong-Cheu Lin*

Department of Materials Science and Engineering, National Chiao Tung University, 1001 Ta Hsueh Road, Hsinchu, Taiwan 30049, ROC

ARTICLE INFO

Article history:
Received 24 July 2009
Received in revised form
23 October 2009
Accepted 24 October 2009
Available online 10 November 2009

Keywords:
Side-chain liquid-crystalline polymer
Atom transfer radical polymerization (ATRP)
Block-copolymer

ABSTRACT

A series of novel side-chain liquid-crystalline polymers (SCLCPs) consisting of laterally attached photoluminescent *p*-quinquephenyl (**QQP**) pendants with different flexible terminal- and/or side-alkoxy chains were synthesized via atom transfer radical polymerization (ATRP). Homopolymers (**HP1**–**HP3**) and block-copolymers (**PSP1**–**PSP3** and **PEOP1**–**PEOP3**), where **QQP** units were copolymerized with styrene or ethylene oxide monomers, possessed the number average molecular weights (M_n) of 8.7–26.0 $\times$ 10^3 with narrow PDI values of 1.08–1.26. Various characterization techniques of polarized optical microscopy (POM), differential scanning calorimetry (DSC), and X-ray diffraction (XRD) were used to investigate their mesomorphic properties, and all homopolymers and block-copolymers exhibited the nematic phase affected by the flexible terminal- and/or side-alkoxy chains of the conjugated rod-like pendants. In addition, the photophysical properties of these polymers were measured by UV–vis and photoluminescence (PL) spectroscopies, which showed blue PL emissions with rather high fluorescence quantum yields in solutions.

1. Introduction

Self-organization into a particular order is a general phenomenon in nature. Block-copolymers (BCPs) present one of the most straightforward models to achieve self-organized nanostructures, which can lead to the formation of a variety of structures such as cylinders, lamellas, and spheres, etc [1]. There are several major classes of synthetic materials that can readily accomplish BCPs with various phase structures, such as amorphous (coil–coil) [2,3], crystalline–amorphous (or crystalline–crystalline) [4–6], and liquid-crystalline (LC) structures [7,8]. LC BCPs have been an active research target in creating different hierarchical structures with unique mesomorphic and mechanical behaviors for several past decades. Numerous LC BCPs have been focused on the LC molecular architectures, which can be divided into main-chain [9–11] and side-chain LC BCPs [12–23], as well as BCPs made of mesogenic jacketed LC polymers (MJLCPs) [24–30]. However, most researches of LC BCPs concentrated on "longitudinally linked" side-chain liquid-crystalline polymers (LCPs) forming a comb-like fashion whose termini of rigid rods in mesogenic units were attached to the polymer backbones through completely flexible spacers [12–23]. Side-chain LCPs consisting of cyanophenyl [12–15], azobenzyl [16–19], and (*n*-alkoxyphenyl)benzyl [20–23] moieties have been usually studied in different applications of mesomorphic, electro-optical, and microphase-separated structural properties, respectively. For example, Yu et al. revealed that well-defined conjugated-LC block-copolymers with side-chain LCPs exhibited the properties that energy transfer from the LC mesogens to the conjugated oligomers [12]. Pugh et al. found that a series of polynorbornenes (PNBEs) laterally attached side-chain LC polymers by using different symmetrically di-substituted mesogens exhibited the tilted layer structure of a smectic C (S_C) phase at room temperature and a nematic (*N*) phase at higher temperatures, which were characterized by polarizing optical microscopy (POM) and X-ray diffraction (XRD) experiments [22]. Based on these concepts, the subject of functional materials can be set more clearly to be explored for new types of block-copolymers with novel mesomorphic and optical properties in this work.

To investigate the structures of LC block-copolymers, many research groups have synthesized several varieties of living or controlled polymerization methods, such as cationic, ring-opening metathesis, and anionic living polymerizations [31–34]. Recently, the controlled ("living") radical polymerizations of atom transfer radical polymerization (ATRP) and nitroxide-mediated radical polymerization have been used to synthesize side-chain LCPs [25–37]. Because the ATRP method can be handled easily and applied to a wide number of monomers and lead to special polymer architectures with narrow polydispersities [38–40], the successful

* Corresponding author. Tel.: +8863 5712121x55305; fax: +8863 5724727.
E-mail addresses: linhc@mail.nctu.edu.tw, linhc@cc.nctu.edu.tw (H.-C. Lin).

0032-3861/$ – see front matter © 2009 Elsevier Ltd. All rights reserved.
doi:10.1016/j.polymer.2009.10.071

polymerization technique was chosen to develop new functional block-copolymers for this research. For instance, a new class of side-on LCP-containing block-copolymers with different hydrophilic/hydrophobic ratios were developed by Li et al. via ATRP method [65].

An approach to increase the rigidity of the polymers, particularly at high temperatures, was to introduce oligo-phenyl segments into the rigid cores of the polymer backbones [41–49]. Thus, the presence of *p*-quinquephenyl (**QQP**) chromophores in the polymer structures was of considerable interest for the creation of new promising multifunctional (including photoluminescent) materials. Besides, such chromophores bearing alkoxy-substituted side groups not only showed increased solubility and high modulus at high temperatures but also exhibited a different phase behavior [44]. For example, Zhou et al. reported that *p*-terphenyl groups with different symmetrical alkoxy terminal substituents exhibited different mesophases, regardless of the lengths of the tails [26]. Furthermore, because of the strong π–π interactions between the conjugated benzene rings favoring the self-organization of molecules, these types of chromophores possessed the multiple properties of photoluminescence, thermally stable liquid crystallinity, and microphase-separated behavior in such systems [45–49].

Herein, we report the synthesis of novel photoluminescent monomers with laterally connected pendent **QQP** moieties substituted by different alkoxy groups at both ends and central sides, the ATRP polymerizations of LC homopolymers and their functional block-copolymers (Chart 1) with narrow polydispersities initiated by different flexible macroinitiators, i.e., poly(ethylene oxide) (**PEO**) and polystyrene (**PS**). The phase transition and mesomorphic properties (investigated by POM, DSC, and temperature-variable XRD) as well as the UV–vis and PL properties of the rod-coil block-copolymers will be evaluated.

2. Experimental

2.1. Measurements

^{1}H NMR spectra were recorded on a Varian Unity 300 MHz spectrometer using $CDCl_3$ and DMSO solvent. Elemental analyses were performed on a HERAEUS CHN-OS RAPID elemental analyzer. Transition temperatures were determined by differential scanning calorimetry (Perkin–Elmer Pyris 7) with a heating and cooling rate of 5 °C/min. Thermogravimetric analysis (TGA) was conducted with a TA instrument Q500 at a heating rate of 20 °C/min under nitrogen. Gel permeation chromatography (GPC) analysis was conducted on a Waters 1515 separation module using polystyrene as a standard and THF as an eluent. UV–vis absorption spectra were recorded in dilute THF solutions (10^{-6} M) on a HPG1103A spectrophotometer, and fluorescence spectra were obtained on a Hitachi F-4500 spectrophotometer, where the excitation wavelengths of PL were ca. 290 nm. Fluorescence quantum yields were determined by using a 9,10-diphenylanthracene standard (10^{-6} M in cyclohexane, $\Phi_F = 90\%$) [50]. Polymer solid films were spin-coated (at 1000 rpm) on quartz substrates for 1 min from THF solutions with a concentration of 10 mg/mL and dried under vacuum at 50 °C for 3 h. LC textures were studied via a polarizing optical microscope (POM, model Leica DMLP) coupled with a hot stage. Synchrotron powder X-ray diffraction (XRD) measurements were performed at beamline BL17A of the National Synchrotron Radiation Research Center (NSRRC), Taiwan, where the wavelength of X-ray was 1.33361 Å. The XRD data were collected using Mar345 image plate detector mounted orthogonal to the beam with sample-to-detector distance of 250 mm, and the diffraction signals were accumulated for 3 min. The powder samples were packed into a capillary tube and heated by a heat gun, whose temperature controller is programmable by a PC with a PID feedback system. The scattering angle theta was calibrated by a mixture of silver behenate and silicon. The self-assembling surface morphology was investigated by the tapping mode of atomic force microscopy (AFM) at room temperature using a Digital Instruments Nanoscope IIIa microscope, where the sample was prepared by dipping a 0.5 wt% copolymer solution (in toluene) onto a Si wafer and then annealed under vacuum at 170 °C for 2 h then cooling slowly to 100 °C for 1 day.

2.2. Materials

Chemicals and solvents were reagent grades and purchased from Aldrich, ACROS, TCI, and Lancaster Chemical Co. Dichloromethane, THF, and triethylamine were distilled to keep anhydrous before use. Catalyst copper (I) bromide was purified successively by stirring in acetic acid and ethanol, and then dried [51]. Styrene monomers were distilled under nitrogen over calcium hydride and 2,6-di(*tert*-butyl-4-methyl)phenol as an inhibitor before use. All of the other chemicals and solvents were used as received.

2.3. Synthesis of polymers

The synthetic routes of macroinitiator **14**–**15** are shown in Scheme S1. Homopolymers (**HP1**–**HP3**) and diblock-copolymers (**PSP1**–**PSP3** and **PEOP1**–**PEOP3**) were synthesized by using the analogous procedure except for the utilization of different initiators and monomers via ATRP in Scheme 1.

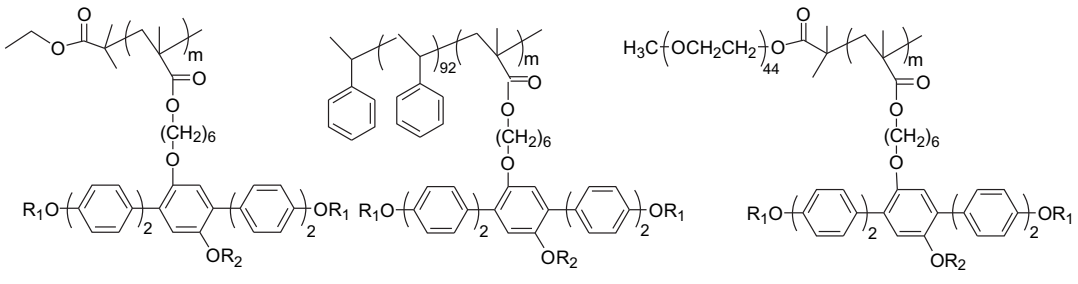

HP1 : $R_1 = C_8H_{17}$; $R_2 = CH_3$
HP2 : $R_1 = C_8H_{17}$; $R_2 = C_8H_{17}$
HP3 : $R_1 = CH_3$; $R_2 = C_8H_{17}$

PSP1 : $R_1 = C_8H_{17}$; $R_2 = CH_3$
PSP2 : $R_1 = C_8H_{17}$; $R_2 = C_8H_{17}$
PSP3 : $R_1 = CH_3$; $R_2 = C_8H_{17}$

PEOP1 : $R_1 = C_8H_{17}$; $R_2 = CH_3$
PEOP2 : $R_1 = C_8H_{17}$; $R_2 = C_8H_{17}$
PEOP3 : $R_1 = CH_3$; $R_2 = C_8H_{17}$

Chart 1. Side-chain liquid-crystalline polymers (SCLCPs) with calamitic LC mesogens.

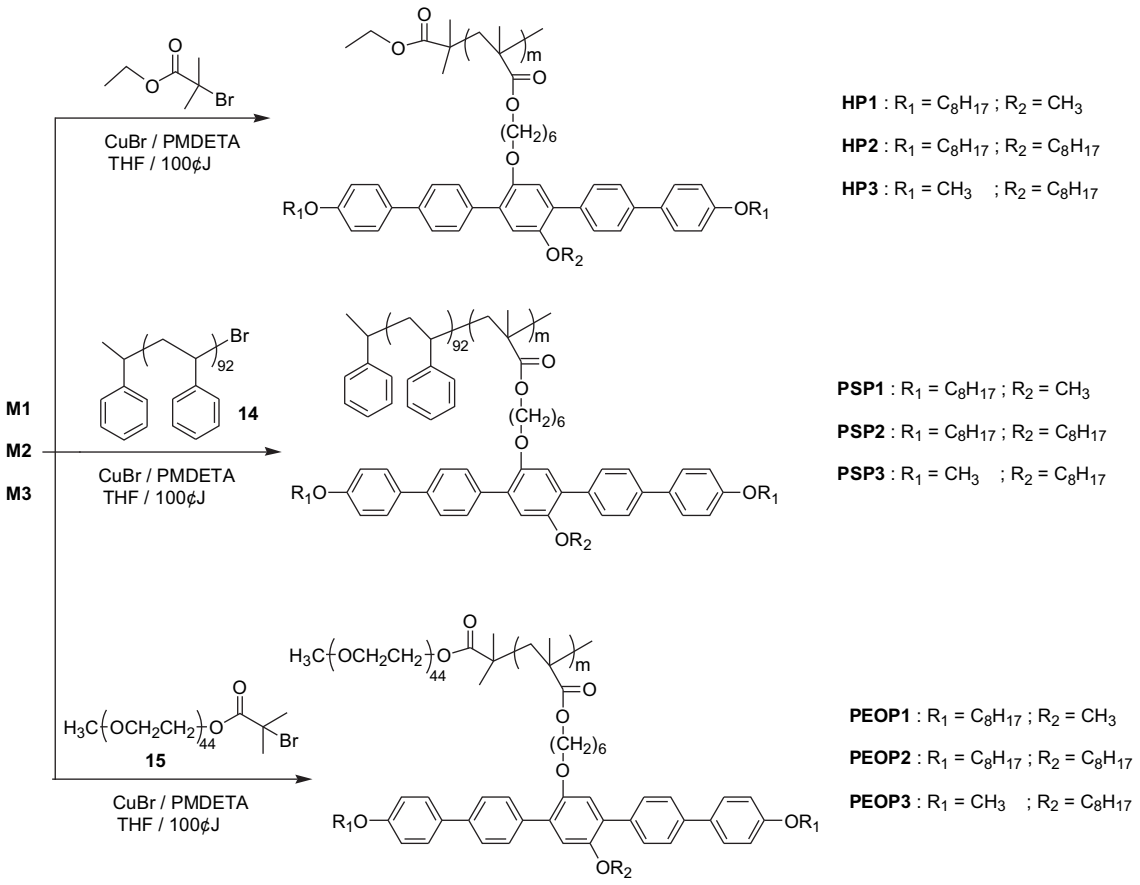

Scheme 1. Synthesis of homopolymers (**HP1**–**HP3**) and diblock-copolymers (**PSP1**–**PSP3** and **PEOP1**–**PEOP3**).

*2.3.1. Macroinitiator polystyrene-Br (**14**)*

In a Schlenk flask, 3.46 mg of *N*,*N*′,*N*′,*N*″-pentamethyldiethylenetriamine (PMDETA, 0.02 mmol), 14.3 mg of CuBr (0.1 mmol), and 5.0 g of styrene (48 mmol) were added and stirred for 30 min. 74 mg of 1-(1-bromoethyl)benzene (0.4 mmol) was added, and the mixture was immediately frozen in liquid nitrogen under vacuum. After several freeze-thaw cycles, the flask was sealed under vacuum and put in an oil bath at 100 °C for 20 h. The content was dissolved in chloroform, and the chloroform solution was precipitated into methanol after being concentrated. The precipitation was repeated three times, and the final product was dried at 50 °C under vacuum. Yield: 55%. $M_n = 9716$ g/mol and PDI (M_w/M_n) = 1.22 (by GPC).

*2.3.2. Macroinitiator **PEO-Br** (**15**)*

A solution of 1.8 g (7.7 mmol) of 2-bromo-2-methylpropionyl chloride in 10 mL of dry THF was added to a mixture of 1.1 g (10 mmol) of triethylamine and 10 g (5 mmol) of poly(ethylene glycol) methyl ether (with $M_n = 2000$) in 30 mL of THF at 0 °C, and then the mixture was stirred for 18 h. After the mixture was filtered, half of the solvent was evaporated, and poly(ethylene glycol) macroinitiator was precipitated into cold ether. After dissolving in ethanol, the solution was stored in refrigerator to re-crystallize to yield a white solid. Yield: 55%. ^{1}H NMR (ppm, $CDCl_3$), δ: 1.94 (s, 6H), 3.38 (s, 3H), 3.54–3.76 (m, 174H), 4.33 (dd, 2H).

*2.3.3. Polymerization of homopolymer **HP1***

7.2 mg (0.05 mmol) of CuBr, 7.4 μL (9.8 mg, 0.05 mmol) of ethyl 2-bromoisobutyrate (EBriB), and 852 mg (1 mmol) of monomer **M1** were mixed and filled with nitrogen. 21 μL (17 mg, 0.1 mmol) of PMDETA in 4 mL of THF was added through a syringe. The mixture was degassed three times using the freeze-pump-thaw procedure and sealed under vacuum. After stirring for 30 min at room temperature, the reaction mixture was placed in a preheated oil bath at 100 °C for 24 h. The solution was passed through a neutral Al_2O_3 column with THF as an eluent to remove the catalyst. The white filtrate was concentrated under reduced pressure and re-precipitated twice into a mixed solvent of EA and methanol (EA/methanol = 1/1). The white product of polymer was collected by filtration and dried under vacuum. Yield: 300 mg (35%). $M_n = 10791$ and PDI (M_w/M_n) = 1.08 (by GPC).

*2.3.3.1. **HP2**.* Homopolymer **HP2** was synthesized according to the procedure described for polymer **HP1** except for the utilization of another monomer **M2**. Yield: 314 mg (33%). $M_n = 10884$ and PDI (M_w/M_n) = 1.08 (by GPC).

*2.3.3.2. **HP3**.* Homopolymer **HP3** was synthesized according to the procedure described for polymer **HP1** except for the utilization of another monomer **M3**. Yield: 241 mg (32%). $M_n = 11358$ and PDI (M_w/M_n) = 1.09 (by GPC).

*2.3.4. Polymerization of block-copolymer **PSP1***

23 mg (0.16 mmol) of CuBr, 388 mg (0.04 mmol) of macroinitiator **14**, and 853 mg (1 mmol) of monomer **M1** were mixed and filled with nitrogen. 83.5 μL (69.3 mg, 0.4 mmol) of PMDETA in 4 mL of THF was added through a syringe. The mixture was degassed three times using the freeze-pump-thaw procedure and sealed under vacuum. After stirring for 30 min at room

temperature, the reaction mixture was placed in a preheated oil bath at 100 °C for 24 h. The solution was passed through a neutral Al_2O_3 column with THF as an eluent to remove the catalyst. The white filtrate was concentrated under reduced pressure and re-precipitated twice into methanol. The white product of polymer was collected by filtration and dried under vacuum. Yield: 307 mg (36%). $M_n = 24380$ and PDI (M_w/M_n) = 1.26 (by GPC).

2.3.4.1. ***PSP2***. Block-copolymer **PSP2** was synthesized according to the procedure described for block-copolymer **PSP1** except for the utilization of another monomer **M2**. Yield: 295 mg (31%). $M_n = 26026$ and PDI (M_w/M_n) = 1.24 (by GPC).

2.3.4.2. ***PSP3***. Block-copolymer **PSP3** was synthesized according to the procedure described for polymer **PSP1** except for the utilization of another monomer **M3**. Yield: 234 mg (31%). $M_n = 24886$ and PDI (M_w/M_n) = 1.21 (by GPC).

2.3.5. Polymerization of block-copolymer ***PEOP1***

23 mg (0.16 mmol) of CuBr, 80 mg (0.04 mmol) of macroinitiator **15**, and 853 mg (1 mmol) of monomer **M1** were mixed and filled with nitrogen. 83.5 μL (69.3 mg, 0.4 mmol) of PMDETA in 4 mL of THF was added through a syringe. The mixture was degassed three times using the freeze-pump-thaw procedure and sealed under vacuum. After stirring for 30 min at room temperature, the reaction mixture was placed in a preheated oil bath at 100 °C for 24 h. The solution was passed through a neutral Al_2O_3 column with THF as an eluent to remove the catalyst. The white filtrate was concentrated under reduced pressure and re-precipitated twice into methanol. The white product of polymer was collected by filtration and dried under vacuum. Yield: 264 mg (31%). $M_n = 10083$ and PDI (M_w/M_n) = 1.10 (by GPC).

2.3.5.1. ***PEOP2***. Block-copolymer **PEOP2** was synthesized according to the procedure described for polymer **PEOP1** except for the utilization of another monomer **M2**. Yield: 275 mg (29%). $M_n = 9884$ and PDI (M_w/M_n) = 1.12 (by GPC).

2.3.5.2. ***PEOP3***. Block-copolymer **PEOP3** was synthesized according to the procedure described for polymer **PEOP1** except for the utilization of another monomer **M3**. Yield: 226 mg (30%). $M_n = 8784$ and PDI (M_w/M_n) = 1.13 (by GPC).

3. Results and discussion

3.1. Synthesis and characterization

The synthetic routes of macroinitiators **14**–**15** and monomers **M1**–**M3** with different alkoxy tail lengths are outlined in Scheme S1. In this work, Suzuki coupling reaction was utilized to prepare the **QQP** (*p*-quinquephenyl) units with different alkoxy tail lengths symmetrically, which has been proven to be very successful in the synthesis of multi-aryl mesogenic systems by Hird et al. [52] ATRP has been proven to be a successful polymerization technique to prepare block-copolymers for a variety of monomers [35–38]. To investigate the properties of block-copolymers containing various LC blocks (composed of monomers **M1**–**M3** with different flexible chain lengths), macroinitiators **14** (with **PS** block) [53] and **15** (with **PEO** block) [54] were used to copolymerize with **M1**–**M3** (bearing laterally attached **QQP** units) to produce LC diblock-copolymers (**PSP1**–**PSP3** and **PEOP1**–**PEOP3**). In addition, homopolymers **HP1**–**HP3** consisting of methacrylate monomers **M1**–**M3** were prepared by using EBriB as an initiator. For all polymerization, polymers were prepared by using CuBr and PMDETA as the catalyst and ligand, and the initial monomer concentration $[M]_0 = 0.25$ M in THF as the reaction conditions were all kept at 100 °C for 24 h, where the specific experimental conditions are also given in Scheme 1 and Table 1.

The relative molecular weights and polydispersity index (PDI) values of the block-copolymers were determined by gel permeation chromatography (GPC) using PS standards, in which THF was used as an eluent. As shown in Table 1, all homopolymers (**HP1**–**HP3**) and diblock-copolymers (**PSP1**–**PSP3** and **PEOP1**–**PEOP3**) had extended molecular weights (M_n = 8784–26026 g mol^{-1}) with narrow PDI values (PDI = 1.08–1.26). The M_n value of macroinitiator **14** obtained by GPC was 9716 g mol^{-1} with a PDI value of 1.28, and macroinitiator **15** was acquired from commercially available **PEO** (M_n = 2000 g mol^{-1}) with PDI = 1.04. The repeat unit (*m* value) of the mesogenic **QQP** block in each polymer can be estimated by subtraction of the first block molecular weight from the final molecular weight measured by GPC and NMR (developed by Yang et al. [65]), and their *m* values are listed in Table 1. Hence, the repeat units (*m* values) of the mesogenic **QQP** blocks in polymers are in the order of diblock-copolymers **PSP1**–**PSP3** > homopolymers **HP1**–**HP3** > diblock-copolymers **PEOP1**–**PEOP3**, and the molecular weights of all polymers also follow the same order of **PSP1**–**PSP3** > **HP1**–**HP3** > **PEOP1**–**PEOP3**.

In this work, all monomers and polymers had good solubility at ambient temperature in common organic solvents, such as THF, EA, and dichloromethane. Since the monomers had poor solubility in methanol, the specially prepared solvent (EA/methanol = 1/1) was chosen to remove un-reacted monomers in the normal precipitation process. The chemical structures of the monomers and block-copolymers were confirmed by ^{1}H NMR spectroscopy, and some representative ^{1}H NMR spectra of monomer (**M1**), homopolymer (**HP1**), and diblock-copolymers (**PSP1** and **PEOP1**) are shown in Fig. S1 of the supporting information. The spectral assignments clearly supported the proposed structures: **M1** showed characteristic proton peaks of the vinyl groups at 5.50–6.06 ppm (denoted as *h* and *i* in Fig. S1(a)), the sharp and clearly separated proton resonances of monomers disappeared after polymerization in Fig. S1(c–d), while broad and overlapped resonances of LC mesogens attached to polymeric backbones appeared at nearly the same positions.

3.2. Thermal properties and phase behavior

The thermal stability of the polymers (**HP1**–**HP3**, **PSP1**–**PSP3** and **PEOP1**–**PEOP3**) was determined by thermogravimetric

Table 1
Molecular weights and yields of ATRP results for homopolymers (**HP1**–**HP3**) and block-copolymers (**PSP1**–**PSP3** and **PEOP1**–**PEOP3**).

Sample	$[M]_0/[I]_0/[C]_0/[L]_0$[a]	M_n[b]	PDI (M_w/M_n)[b]	*m* (repeat unit of **QQP** mesogens)[c]	Yield (%)
HP1	20/1/1/2	10791	1.08	13	35
HP2	20/1/1/2	10884	1.08	11	33
HP3	20/1/1/2	11358	1.09	15	32
PSP1	25/1/4/10	24380[d]	1.26	17	36
PSP2	25/1/4/10	26026[d]	1.24	17	31
PSP3	25/1/4/10	24886[d]	1.21	20	31
PEOP1	25/1/4/10	10083[e]	1.10	9	31
PEOP2	25/1/4/10	9884[e]	1.12	8	29
PEOP3	25/1/4/10	8784[e]	1.13	9	30

[a] Feed molar ratio; [M], monomer; [I], initiator; [C], catalyst; [L], ligand.
[b] Molecular weights and polydispersity index (PDI) values were measured by GPC, using THF as an eluent, polystyrene as a standard. M_n, number average molecular weight; M_w, weight average molecular weight.
[c] m values are based on the number average molecular weights M_n measured by GPC. Molecular weights of **M1**–**M3** are 852, 950, and 754 g/mol, respectively.
[d] As measured by GPC, the number average molecular weight (M_n) of the **PS** block (macroinitiator **14**) was 9716 g/mol.
[e] As acquired from commercially available **PEO**, the number average molecular weight (M_n) of the **PEO** block (macroinitiator **15**) was 2000 g/mol.

analysis (TGA) under nitrogen, which indicated that all polymers exhibited the degradation temperatures (T_d) higher than 375 °C (5% weight loss under nitrogen, as shown in Table 2). Generally, the T_d values of three series homopolymers and block-copolymers could be roughly differentiated by the side-chain molecular components. The T_d values of homopolymers (**HP1**–**HP3**) were slightly higher than those of block-copolymers (**PSP1**–**PSP3** and **PEOP1**–**PEOP3**) even if the molecular weights of **PSP1**–**PSP3** were larger than those of **HP1**–**HP3**. This is due to the rigid molecular arrangements from the single side-chain moiety in homopolymer system. However, the molecular arrangement was dispersed slightly by the introduction of block moieties **PS** and **PEO**, and the T_d values of block-copolymers **PSP1**–**PSP3** and **PEOP1**–**PEOP3** were reduced. To compare the T_d values in the identical series of polymers, polymers bearing longer lateral-alkoxy chains (**HP3**, **PSP3**, and **PEOP3**) exhibited lower T_d values [64]. The phase and glass transition temperatures of all polymers were characterized by polarizing optical microscopy (POM) and DSC traces (the seconding heating and first cooling scans), which are illustrated in Table 2 and Figs. S2 and S3 of the supporting information. The mesophases of diblock-copolymers were also confirmed by POM, for instance, homopolymer **HP1** displayed the nematic phase with dark threads by cooling the sample below the clearing temperature (T_{NI} = 135 °C) as shown in Fig. S3. All polymers illustrated the nematic phase which were adopted from the mesomorphic properties of **QQP** units. The ranges of the nematic phase for all polymers are in the order of polymer series **1** (polymers containing monomers **M1**) > **3** (polymers containing monomers **M3**) > **2** (polymers containing monomers **M2**), which could be realized by the trend of the similarity in rod-like shape for calamitic LC mesogens in monomers: **M1** > **M3** > **M2**. Hence, it can be realized that the long peripheral flexible chains (–OC_8H_{17}) on both longitudinal termini and lateral sides of the rigid pendent rods would interfere with the rod-like shape in the molecular architectures of **M2** and its related polymer series **2** (i.e., **HP2**, **PSP2**, and **PEOP2** containing **M2**), and thus to be detrimental to their mesophase and have the narrowest nematic LC ranges in all polymers. Furthermore, the mesomorphic properties of block-copolymers **PSP1**–**PSP3** and **PEOP1**–**PEOP3** were compared with those of homopolymers **HP1**–**HP3**. Due to the disturbance of the other non-mesogenic coil-blocks of **PS** and **PEO** was surveyed, and the mesophasic ranges of all polymers follows the order of: homopolymers (**HP1**–**HP3**) > block-copolymers (**PSP1**–**PSP3** with larger ***m*** values and longer **QQP** blocks) > block-copolymers (**PEOP1**–**PEOP3** with smaller m values and shorter **QQP** blocks), respectively.

Glass transition temperatures (T_g) of polymer series **1** and **3** containing monomers **M1** and **M3** (except **PEOP3**) were easy to be identified in DSC results, which are in the range of 60–77 °C. However, glass transition temperatures of polymer series **2** containing monomer **M2** are not detectable as the alkoxy groups on the terminal ends and lateral sides were all elongated to octyloxy (–OC_8H_{17}) chains, but sharper melting peaks were observed in this series. Except for two endothermic transitions (including the respective crystal-nematic and nematic-isotropic phase transitions) observed in polymer series **2** containing monomer **M2**, all block-copolymers displayed a nematic-isotropic phase transition endotherm, which were similar to homopolymers (**HP1**–**HP3**) containing LC **QQP** units. Because of the smallest molecular weights and shortest **QQP** blocks of block-polymers **PEOP1**–**PEOP3** in corresponding polymers, the lowest isotropization temperatures were observed in Table 2. For example, T_{NI} of **PEOP1** (131.7 °C) was lower than those of **HP1** and **PSP1** (151.4 and 139.4 °C, respectively). However, even though **PS** block-copolymers had much higher molecular weights and longer **QQP** blocks than homopolymers, block-copolymers **PSP1**–**PSP3** had lower isotropization temperatures than homopolymers **HP1**–**HP3**. It could be owing to the decreased stability of the mesophases by connecting PS block in the micro-domain architectures of the diblock-copolymers. In addition, the lowest isotropization temperatures of polymer series **2** containing monomer **M2** were observed in comparison with those of analogous polymers in series **1** and **3** (see Table 2). Furthermore, an interesting point of the DSC results is that the enthalpies of both endothermic and exothermic transitions were similar and small. Compared with the conventional transition enthalpy changes of low ordered N, S_A, or S_C phase to isotropic phase, the DSC results in Table 2 are quite smaller [56,57]. It could be suggested that if the thermal behavior is correlated to an order–disorder transition attributed to the supramolecular structure change, such as block-copolymers in colloids, and the transition detected by DSC must be associated with a small change of molecular interactions (an enthalpy term) [58,59].

Table 2
Phase behavior and thermal properties of homopolymers and block-copolymers.

Sample	Phase transitions (°C)[a,b] (corresponding enthalpy changes, J g^{-1})		T_g (°C)[a]	T_d (°C)[c]
	Heating	Cooling		
HP1	g 63.3 N 151.4 (0.8) I	I 149.3 (−1.0) N	63.3	391
HP2	Cr 97.5 (19.6) N 107.7 (1.0) I	I 106.6 (−1.2) N 62.4 (−9.5) Cr	nd[e]	391
HP3	g 60 N 128.7 (0.8) I	I 127.4 (−1.3) N	60.0	378
PSP1	g 65 N 139.4 (0.6) I	I 138.2 (−0.6) N	65.0	386
PSP2	Cr 90.2 (5.4) N 97.7 (0.7) I	I 96.7 (−0.8) N	nd[e]	387
PSP3	g 77.3 N 126.5 (0.6) I	I 123.9 (−0.6)	77.3	380
PEOP1	g 65.4 N 131.7 (0.6) I	I 130.9 (−0.5) N 117.2 (−0.2) Cr	65.4	379
PEOP2	Cr 93.4 (11.3) N 98.8 (0.6) I	I 97.6 (−0.7) N 62.4 (−6.4) Cr	nd[e]	381
PEOP3	Cr 95.0[d] N 104.9 (0.4) I	I 103.4 (−0.4) N	nd[e]	375

[a] Transition temperatures (°C) and enthalpies (in parentheses, J g^{-1}) were measured by DSC (at a heating and cooling rate of 5 °C/min).
[b] Cr = crystalline; N = nematic phase; I = isotropic phase.
[c] Temperature (°C) at 5% weight loss measured by TGA at a heating rate of 20 °C/min under nitrogen.
[d] Determined by POM.
[e] nd = Not detected.

3.3. X-ray measurements

To further identify the phase behavior revealed by DSC and POM measurements, X-ray diffraction (XRD) experiments were carried out to give more mesomorphic properties of molecular packings. Fig. S4 of the supporting information shows the plots of X-ray intensity (I) versus angle (2θ) for some examples of polymer series 2 (i.e., **HP2**, **PSP2**, and **PEOP2**). Hence, the wide-angle X-ray studies on polymer samples supported more definitive information about the nematic liquid-crystalline phase. Irrespective of chain architectures in homopolymers **HP2** or block-copolymers **PSP2** and **PEOP2**, all polymers possessed almost identical XRD patterns, which were not affected by the coil-blocks of **PS** and **PEO** units in the block-copolymers **PSP2** and **PEOP2**. Regardless of the lengths of mesogenic **QQP** units with either long tails (–OC_8H_{17}) or short tails (–OCH_3), the XRD results of all polymers showed a broad wide-angle peak around 2θ = 16–17° (correlated to $d \sim 4.7$ Å), which corresponded to the intermolecular distance between the mesogenic units. Moreover, different longitudinally linked side-chain liquid-crystalline block-copolymers in our previous report also showed a similar broad wide-angle peak around 2θ = 16–17° (correlated to $d \sim 4.5$ Å) to illustrate the intermolecular distance between the mesogenic units of the smectgens. [14,63] This interesting result suggested that the compactness of lateral packing of

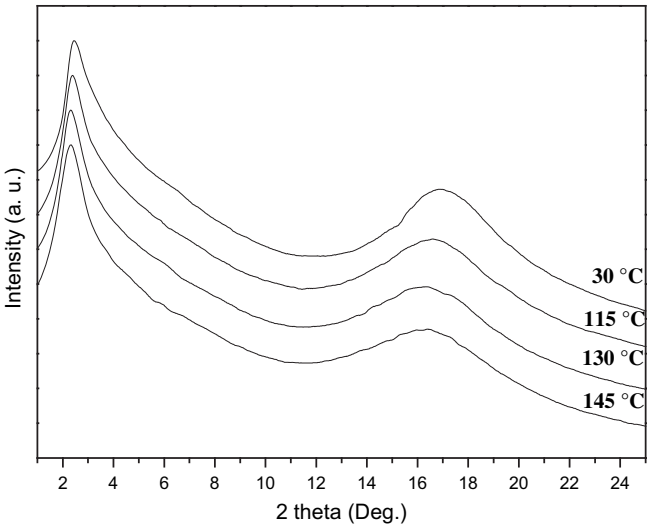

Fig. 1. X-ray diffraction (XRD) patterns of polymer **HP1** at various temperatures during the heating scan.

polymer backbones does not seriously affect this correlation length between mesogens in different mesophases.

Another important result is that Fig. S4 demonstrates another moderate sharper peak at the low-angle region around $2\theta = 2$–3° (correlated to $d = 25$–38 Å). However, the nematic liquid-crystalline phase of longitudinally linked side-chain liquid-crystalline copolymers in our previous reports did not show the low-angle peak [20,60]. These low-angle XRD peaks in Fig. S4 were related to the interchain packing distance of the polymer backbones induced by the jacket-like arrangements of mesogens in the nematic phase, and similar phenomena were also observed in the previously reported mesogenic jacketed LC polymers (MJLCPs) [61,62]. Therefore, the low-angle XRD peaks of homopolymers **HP2** ($2\theta = 2.39^\circ$), block-copolymers **PSP2** ($2\theta = 2.21^\circ$), and **PEOP2** ($2\theta = 2.30^\circ$) in Fig. S4 had the *d*-spacing values in the sequence of **HP2** < **PEOP2** < **PSP2**, because the coil-blocks of **PEO** and **PS** units in block-copolymers **PEOP2** and **PSP2** would expand the interchain packing distance of the polymer backbones to different extents. Moreover, in contrast to the low-angle XRD peaks at $2\theta = 4.9$–5.1° (correlated to $d = 18.0$–17.2 Å) for MJLCPs reported in Refs. 61 and 62, another evidence of the larger interchain packing distance ($d = 38$–25 Å) of the polymer backbones in our polymers (**HP2**, **PSP2**, and **PEOP2**) were revealed owing to our longer spacers (i.e., CO–O–C_6H_{12}–O) between the polymer backbones and mesogenic units. Furthermore, due to thermal expansion of the interchain packing distance of the polymer backbones and the intermolecular distance between mesogenic units, both low- and wide-angle XRD peaks of homopolymer **HP1** in Fig. 1 shifted slightly to smaller 2θ angles (correlated to larger d-spacing values) upon heating. The relative orientation of side groups versus the backbones should determine the mesophasic structures of the polymers. In our systems, these side-chain polymers with laterally attached rigid rod-like mesogenic groups exhibited remarkable differences in phase behavior from conventional SCLCPs on the basis of flexible or semiflexible backbones, suggesting the formation a nematic liquid-crystalline phase.

Table 3
Absorption and PL emission spectral data of polymers in THF solutions and solid films.

Sample	Absorption λ_{abs} (nm)		PL emission λ_{max} (nm)		Φ (Solution)[b]
	Solution[a]	Solid film	Solution[a]	Solid film	
HP1	292, 332	292, 340	404	407	0.76
HP2	287, 332	287, 343	405	406	0.67
HP3	292, 333	292, 340	404	407	0.65
PSP1	286, 332	286, 339	404	408	0.72
PSP2	288, 333	288, 342	405	407	0.69
PSP3	288, 328	288, 339	405	407	0.68
PEOP1	288, 332	288, 341	404	407	0.68
PEOP2	287, 333	287, 341	404	406	0.51
PEOP3	287, 333	287, 342	404	406	0.70

[a] Absorption and PL emission spectra were measured in THF solutions at room temperature, where the excitation wavelengths of PL were ca. 290 nm.
[b] Fluorescence quantum efficiencies of solutions were measured in THF, relative to 9,10-diphenylanthracene ($\Phi_{PL} = 0.90$).

3.4. Optical properties

The UV–vis absorption and photoluminescence (PL) data of polymers **HP1**–**HP3**, **PSP1**–**PSP3**, and **PEOP1**–**PEOP3** were measured in both solutions (ca. 1×10^{-6} M in dilute solutions of good solvent THF) and solids, where the excitation wavelengths of PL were ca. 290 nm, and the photophysical properties are summarized in Table 3. As shown in Fig. 2, **HP1**–**HP3** possessed almost identical UV–vis absorption and PL spectra. Thus, two maxima were obtained in the absorption spectra: the one at ca. 332 nm was a typical peak for substituted quinquephenyl moieties [55,61], and the other one at ca. 287 nm was a superposition absorption band originated from the quinquephenyl unit. In the PL

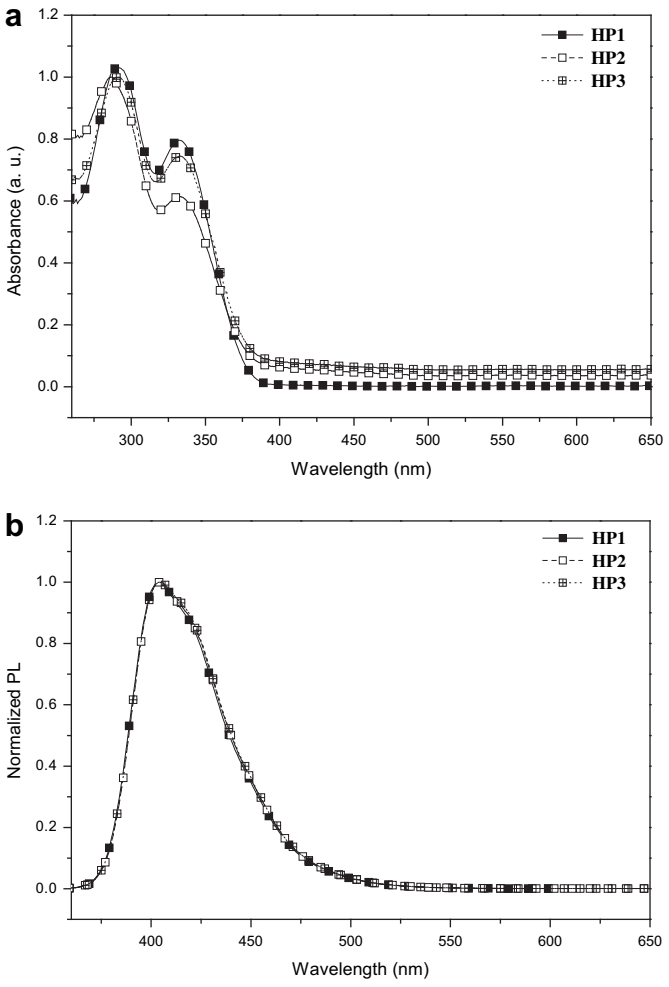

Fig. 2. Normalized (a) UV–vis absorption spectra and (b) PL spectra of homopolymers **HP1**–**HP3** in THF solutions.

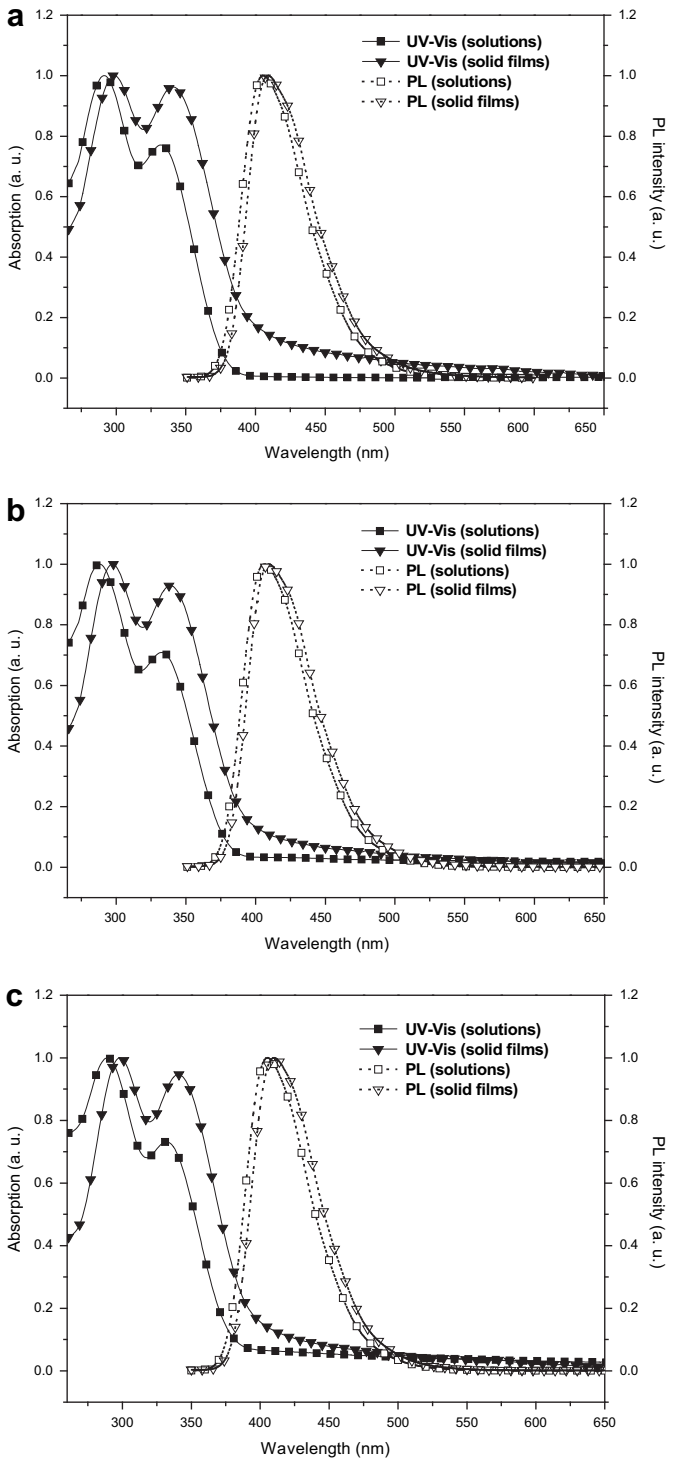

Fig. 3. (—) UV–vis absorption and (- - -) PL spectra of (a) **HP1**, (b) **PSP1**, and (c) **PEOP1** in THF solutions and solid films.

spectra, a blue fluorescence maxima at ca. 404 nm and a shoulder at ca. 420 nm were observed, which belong to PL emission characteristics of the quinquephenyl moiety [55,61]. As shown in Table 3, all polymers showed blue PL emissions with rather high fluorescence quantum yields in solutions. Fig. 3 shows the examples of UV–vis and PL spectra of homopolymer **HP1** and diblock-copolymers **PSP1** and **PEOP1**. Compared with the UV–vis absorption and PL spectra in THF solutions, the polymers exhibit minor red-shifted effects in solid films, because of the intermolecular π–π^* aggregation of the rigid cores in photoluminescent quinquephenyl blocks. In contrast to analogous homopolymers, most corresponding block-copolymers possessed UV–vis absorption maxima with 0–6 nm blue shifts in both solutions and solid films, which might be associated with minor dilution effect of coil-blocks in block-copolymers, and much less blue shifts occurred in polymer series **2** due to the longer peripheral flexible chains ($-OC_8H_{17}$) around luminescent chromophore units of **M2**. Nevertheless, due to the same explanation of minor dilution effect of coil-blocks in block-copolymers, no obvious variations in PL emission maxima and fluorescence quantum yields were achieved between analogous homopolymers and block-copolymers. In general, UV–vis absorption and PL spectra of all polymers are quite similar, which are mainly due to the similar photoluminescent rigid cores of quinquephenyl blocks (even with different flexible alkoxy lengths).

3.5. AFM investigation of self-assembling nanostructures

In order to investigate the self-assembling property of the diblock-copolymers, the surface morphology was measured by AFM as shown in Fig. 4. Due to the incompatibility of hydrophilic **PEO** segments and hydrophobic parts (five-ring rigid cores) in diblock-copolymers, the flexible **PEO** segments of polymer **PEOP3** could be self-aggregated in toluene due to the insoluble parts of hydrophilic **PEO** segments. As shown in the AFM image, the morphological image presents individual spherical micelles and the core–shell model. The phenomenon of globularity protrusion was obtained and dispersed like the short uninterrupted serpentine pinnacle, which meant the rigid segment of mesogenic rods in **PEOP3**, and the high-profile (bright) area was indicative of the soft segments of **PEO** polymer chains (insoluble parts in toluene). As shown in Fig. 4, the diameter of the aggregated observation in the AFM image was about 200 nm which is rather heterogeneous depending on the block composition. These results clearly demonstrate the effect of block-copolymer composition on the micellar dimensions. Although **QQP** chains compared with **PEO** coils are shorter, the molecular volume fraction of the rod blocks in monomers is larger, resulting in a larger number of aggregation for the micelles and hence self-assembled into larger micelles. These results indicate that the well-documented scaling laws established for block-copolymer micelles are in agreement with the core size

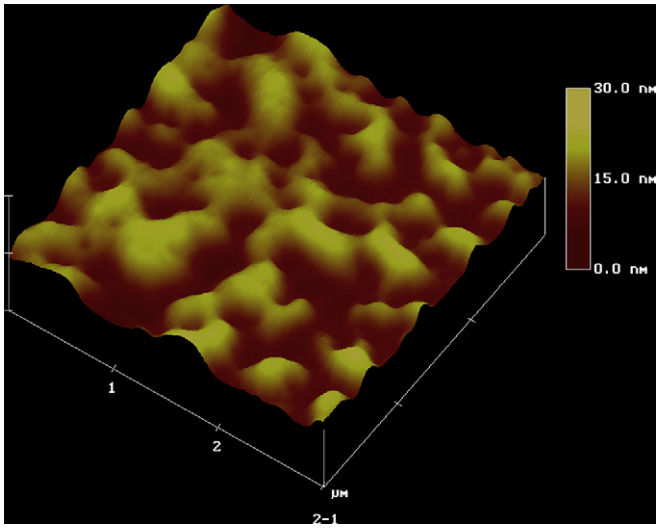

Fig. 4. AFM image of the self-assembled nanostructure of copolymer **PEOP3** (from toluene).

with respect to the total size, and the number of aggregation mainly depend on the degree of polymerization of the rod blocks.

4. Conclusions

In summary, a series of novel side-chain liquid-crystalline polymers (SCLCPs) were made of laterally attached photoluminescent *p*-quinquephenyl (**QQP**) monomers containing flexible terminal- and/or side-alkoxy chains via Suzuki coupling reactions in this research. Using monofunctional polystyrenes and poly(ethylene oxide)s as macroinitiators, **QQP**-based macromolecular architectures such as homopolymers and diblock-copolymers with $2.6 \times 10^4 \geq M_n \geq 8.8 \times 10^3$ and narrow polydispersity index (PDI) values ($1.26 \geq M_w/M_n \geq 1.08$) could be successfully synthesized by atom transfer radical polymerization (ATRP). The nematic LC phase was further confirmed to exist in all homopolymers and copolymers, which were influenced by the long peripheral flexible chains ($-OC_8H_{17}$) on both longitudinal termini and lateral sides of the rigid pendent rods. Thus, the ranges of the nematic phase for all polymers are in the order of polymer series **1** (polymers containing monomers **M1**) > **3** (polymers containing monomers **M3**) > **2** (polymers containing monomers **M2**), which could be comprehended by the degree of the similarity in rod-like shape for calamitic LC mesogens in monomers: **M1** > **M3** > **M2**. Furthermore, due to the disturbance of the other non-mesogenic coil-blocks of **PS** and **PEO** units, the mesophasic ranges of all polymers follows the order of: homopolymers (**HP1**–**HP3**) > block-copolymers (**PSP1**–**PSP3** with larger *m* values and longer **QQP** blocks) > block-copolymers (**PEOP1**–**PEOP3** with smaller *m* values and shorter **QQP** blocks), respectively. Besides mesomorphic properties, all polymers had almost identical maximum UV–vis absorption and blue PL emission wavelengths originated from their similar rod-like conjugated units in dilute solutions and solid films, but a red-shifted effect in solid films occurred due to intermolecular π–π^* aggregation of the rigid cores. The nematic (*N*) phase was also proven by XRD patterns so that the low-angle XRD peaks ($2\theta = 2$–3°) were related to the interchain packing distance of the polymer backbones induced by the jacket-like arrangements of mesogens in the nematic phase. The wide-angle XRD peaks ($2\theta = 16$–17°) illustrated the intermolecular distance between the mesogenic units. Therefore, the mesomorphic and photophysical properties of the corresponding LC homopolymers and block-copolymers with laterally attached photoluminescent mesogenic units were first explored here.

Acknowledgements

The powder XRD measurements are supplied by beamline BL17A (charged by Dr. Jey-Jau Lee) of the National Synchrotron Radiation Research Center (NSRRC), in Taiwan. The instruments of GPC measurements were provided by Prof. Kung-Hwa Wei (Dept. of Materials Science & Engineering, National Chiao Tung University).

Appendix. Supplementary data

Supplementary data associated with this article can be found in the online version, at doi:10.1016/j.polymer.2009.10.071.

References

[1] Park C, Yoon J, Thomas EL. Polymer 2003;44:6725.
[2] Bates FS. Science 1991;251:898.
[3] Lecomte HA, Liggat JJ, Curtis ASG. J Polym Sci Part A Polym Chem 2006;44:1785.
[4] Uehara H, Takeuchi KI, Kakiage M, Yamanobe T, Komoto T. Macromolecules 2007;40:5820.
[5] Yoshida T, Seno KI, Kanaoka S, Aoshima S. J Polym Sci Part A Polym Chem 2005;43:1155.
[6] Serhatli IE, Kacar T, Önen A. J Polym Sci Part A Polym Chem 2003;41:1892.
[7] Zhang L, Yu K, Eisenberg A. Science 1996;272:1777.
[8] Muthukumar M, Ober CK, Thomas EL. Science 1997;277:1225.
[9] Ojha UP, Kumar A. J Polym Sci Part A Polym Chem 2006;44:3479.
[10] Lin HC, Lee KW, Tsai CM, Wei KH. Macromolecules 2006;39:3808.
[11] Ribera D, Giamberini M, Serra A, Mantecón A. J Polym Sci Part A Polym Chem 2006;44:6270.
[12] Yu XF, Lu S, Ye C, Li T, Liu T, Liu S, et al. Macromolecules 2006;39:1364.
[13] Yu H, Shishido A, Ikeda T, Iyoda T. Macromol Rapid Commun 2005;26:1594.
[14] Lee KW, Wei KH, Lin HC. J Polym Sci Part A Polym Chem 2006;44:4593.
[15] Oriol L, Piñol M, Serrano JL, Alcalá MR, Cases AR, Sánchez C. Polymer 2001;42:2737.
[16] Morikawa Y, Kondo T, Nagano S, Seki T. Chem Mater 2007;19:1540.
[17] Tang X, Gao L, Fan XH, Zhou QF. J Polym Sci Part A Polym Chem 2007;45:2225.
[18] (a) Forcén P, Oriol L, Sánchez C, Alcalá R, Hvilsted S, Jankova K, et al. J Polym Sci Part A Polym Chem 2007;45:1899;
(b) Tang X, Gao L, Han N, Fan X, Zhou Q. J Polym Sci Part A Polym Chem 2007;45:3342.
[19] (a) He X, Sun W, Yan D, Xie M, Zhang Y. J Polym Sci Part A Polym Chem 2008;46:4442;
(b) Zhang Y, Zhang W, Chen X, Cheng Z, Wu J, Zhu J, et al. J Polym Sci Part A Polym Chem 2008;46:777.
[20] Lee KW, Lin HC. J Polym Sci Part A Polym Chem 2007;45:4564.
[21] Lee KW, Lin HC. Polymer 2007;48:3664.
[22] (a) Pugh C, Zhu P, Kim G, Zheng JX, Rubal MJ, Cheng SZD. J Polym Sci Part A Polym Chem 2006;44:4076;
(b) Kim GH, Pugh C, Cheng SZD. Macromolecules 2000;33:8983.
[23] Qiao WQ, Fan XD, Kong J, Xie YC, Si QF, Wang SJ, et al. J Polym Sci Part A Polym Chem 2005;43:3067–78.
[24] (a) Xie H, Hu T, Zhang X, Zhang H, Chen E, Zhou QF. J Polym Sci Part A Polym Chem 2008;46:7310;
(b) Ying W, Zheng JX, Brittain WJ, Cheng SZD. J Polym Sci Part A Polym Chem 2006;44:5608.
[25] (a) Chen S, Gao LC, Zhao XD, Chen XF, Fan XH, Xie PY, et al. Macromolecules 2007;40:5718;
(b) Liu LB, Hong DJ, Lee M. Langmuir 2009;25:5061.
[26] (a) Yu Z, Tu H, Wan X, Chen X, Zhou QF. J Polym Sci Part A Polym Chem 2003;41:1454;
(b) Kieffer R, Prehm M, Pelz K, Baumeister U, Liu F, Hahn H, et al. Soft Matter 2009;5:1214.
[27] (a) Tu H, Yu Z, Wan X, Li L, Sun L, Chen X, et al. Macromol Symp 2001;164:347;
(b) Moughton AO, Stubenrauch K, O'Reilly RK. Soft Matter 2009;5:2361.
[28] (a) Zhu Z, Zhi J, Liu A, Cui J, Tang H, Qiao W, et al. J Polym Sci Part A Polym Chem 2007;45:830;
(b) Zhi JG, Guan Y, Cui JX, Liu AH, Zhu ZG, Wan XH, et al. J Polym Sci Part A Polym Chem 2009;47:2408.
[29] (a) Sun LM, Fan XH, Chen XF, Liu XF, Zhou QF. J Polym Sci Part A Polym Chem 2007;45:2543;
(b) Cui JX, Liu AH, Zhi J, Zhu ZG, Guan Y, Wan XH, et al. Macromolecules 2008;41:5245.
[30] (a) Tang H, Zhu Z, Wan X, Chen XF, Zhou QF. Macromolecules 2006;39:6887;
(b) Zeng XB, Liu F, Fowler AG, Ungar G, Cseh L, Mehl GH, et al. Adv Mater 2009;21:1746.
[31] Shibata T, Kanaoka S, Aoshima S. J Am Chem Soc 2006;128:7497.
[32] Han H, Chen F, Yu J, Dang J, Ma Z, Zhang Y, et al. J Polym Sci Part A Polym Chem 2007;45:3986.
[33] (a) Crivello JV. J Polym Sci Part A Polym Chem 2007;45:3759;
(b) Ruan JJ, Jin S, Ge JJ, Jeong KU, Graham MJ, Zhang D, et al. Polymer 2006;47:4182.
[34] Biagini SCG, Parry AL. J Polym Sci Part A Polym Chem 2007;45:3178.
[35] (a) Tsarevsky NV, Matyjaszewski K. Chem Rev 2007;107:2270;
(b) Matyjaszewski K, Xia J. Chem Rev 2001;101:2921;
(c) Kamigaito M, Ando T, Sawamoto M. Chem Rev 2001;101:3689.
[36] Ajioka N, Suzuki Y, Yokoyama A, Yokozawa T. Macromolecules 2007;40:5294.
[37] Jiaming Z, Rui L, Jianying H, Jiayan C, Xurong L, Yutai L, et al. J Polym Sci Part A Polym Chem 2007;45:4082.
[38] Thakur S, Tillman ES. J Polym Sci Part A Polym Chem 2007;45:3488.
[39] (a) Limer A, Haddleton DM. Macromolecules 2006;39:1353;
(b) Xue L, Agarwal US, Zhang M, Staal BBP, Müller AHE, Bailly CME, et al. Macromolecules 2005;38:2093.
[40] Mittal A, Sivaram S. J Polym Sci Part A Polym Chem 2005;43:4996.
[41] Perez-Velasco A, Gorteau V, Matile S. Angew Chem Int Ed 2008;47:921.
[42] Kishore RSK, Ravikumar V, Bernardinelli G, Sakai N, Matile S. J Org Chem 2008;73:738.
[43] (a) Spiliopoulos IK, Mikroyannidis JA. J Polym Sci Part A Polym Chem 2002;40:682;
(b) Spiliopoulos IK, Mikroyannidis JA. J Polym Sci Part A Polym Chem 2002;40:2591;
(c) Vellis PD, Mikroyannidis JA, Cho MJ, Choi DH. J Polym Sci Part A Polym Chem 2008;46:5592.
[44] (a) Kakali F, Gravalos KG, Kallitsis JK. J Polym Sci Part A Polym Chem 1996;34:1581;

(b) Economopoulos SP, Chochos CL, Gregoriou VG, Kallitsis JK, Barrau S, Hadziioannou G. Macromolecules 2007;40:921.
[45] Lin HC, Tsai CM, Huang GH, Lin JM. J Polym Sci Part A Polym Chem 2006;44:783.
[46] Pistolis G, Andreopoulou AK, Malliaris A, Kallitsis JK. Macromolecules 2004;37:1524.
[47] Mikroyannidis JA, Stylianakis MM, Sharma GD, Bahraju P, Roy MS. J Phys Chem C 2009;113:7904.
[48] Riala P, Andreopoulou A, Kallitsis J, Gitsas A, Floudas G. Polymer 2006;47:7241.
[49] Pefkianakis EK, Tzanetos NP, Chochos CL, Andreopoulou AK, Kallitsis JK. J Polym Sci Part A Polym Chem 2009;47:1939.
[50] Hamai S, Hirayama F. J Phys Chem 1983;87:83.
[51] Neugebauer D, Matyjaszewski K. Macromolecules 2003;36:2598.
[52] Hird M, Gray GW, Toyne KJ. Mol Cryst Liq Cryst 1991;206:187.
[53] Cui L, Zhao Y, Yavrian A, Galstian T. Macromolecules 2003;36:8246.
[54] Tian Y, Watanabe K, Kong X, Abe J, Iyoda T. Macromolecules 2002;35:3739.
[55] Kallitsis JK, Gravalos KG, Hilberer A, Hadziioannou G. Macromolecules 1997;30:2989.
[56] Keller A, Cheng SZD. Polymer 1998;39:4461.
[57] Chien W, Wunderlich B. Macromol Chem Phys 1999;200:283.
[58] Ungar G, Feijoo JL, Percec V, Tound R. Macromolecules 1991;24:953.
[59] Zhao YF, Fan XH, Wan XH, Chen XF, Yi Y, Wang LS, et al. Macromolecules 2006;39:948.
[60] Liang TC, Lin HC. J Polym Sci Part A Polym Chem 2009;47:2734.
[61] Pragliola S, Ober CK, Mather PT, Jeon HG. Macromol Chem Phys 1999;200:2338.
[62] Gopalan P, Zhang Y, Li X, Wiesner U, Ober CK. Macromolecules 2003;36:3357.
[63] (a) Li XG, Huang MR. Angew Makromol Chem 1995;227:69;
(b) Li XG, Huang MR, Guan GH, Sun T. Angew Makromol Chem 1997;249:93.
[64] (a) Li XG, Huang MR, Guan GH, Sun T. Polym Int 1998;46:289;
(b) Li XG, Huang MR. Polym Degrad Stab 1999;64:81.
[65] Yang J, Pinol R, Gubellini F, Levy D, Albouy PA, Keller P, et al. Langmuir 2006;22:7907.